

Supplement of Atmos. Chem. Phys., 17, 14119–14143, 2017
<https://doi.org/10.5194/acp-17-14119-2017-supplement>
© Author(s) 2017. This work is distributed under
the Creative Commons Attribution 3.0 License.



Supplement of

Long-path measurements of pollutants and micrometeorology over Highway 401 in Toronto

Yuan You et al.

Correspondence to: Ralf M. Staebler (ralf.staebler@canada.ca)

The copyright of individual parts of the supplement might differ from the CC BY 3.0 License.

S1. Description of spectrum fitting method

As mentioned in the main text, high resolution reference spectra were taken from the HITRAN database at 296 K and 101325 Pa when available. For species not available in the HITRAN database, the reference spectra were taken from the PNNL database at 25 °C. Before measurements, the wavenumber calibration was performed by fitting a function for the instrumental line shape (ILS) (Harig et al., 2005). The ILS function also takes the reference spectra and calculates reference spectra into spectra with the same spectral resolution, 0.5 cm^{-1} in our case. A known gas is selected, water H_2O in our case, and a spectral range is fitted by adjusting ILS parameters.

As described in the main text, “at the beginning of the measurement period, a stray light spectrum was recorded by pointing the spectrometer away from the retroreflector. This stray light spectrum accounts for radiation back to the detector from reflections by internal parts inside the spectrometer, i. e. not from the retroreflector array, and was subtracted from all the measurement spectra before performing further analysis.” The software which collects spectra and does spectral fitting analysis is called OPUS_RS. OPUS_RS calculates the spectral fitting by a non-linear curve fitting algorithm. Spectral fitting analysis was mainly done in the process of making reference files for each pollutant. Spectral windows/regions and interference gases for each gases were determined by examining the reference spectrum and picking the absorption features. Spectral windows in previous studies were also examined and adjusted to get a good fit. For CO , CO_2 , N_2O , HCN , HCHO , and NH_3 , we used spectral regions reported in previous studies (showing in Table 1 in the main text), since the fittings were good. It was also critical to include interference gases relevant in the spectral window under analysis. After many rounds of adjusting windows and interfering gases, an “optimized fit” was determined by examining the measurement spectrum, fitted spectrum, correlation coefficients and residuals. To further improve fittings, baseline calculations were performed under given spectral windows and interfering gases. Three methods are included in the baseline algorithm of the OPUS_RS software: offset, linear baseline correction, and standard baseline algorithm. “Offset” and “linear baseline correction” provide a linear baseline calculation, and they were used when the base of the spectral region was roughly straight. The “standard baseline correction” algorithm uses Gaussian functions to simulate the baseline. It has two parameters: distance and width (both in cm^{-1}). “Distance” controls how far apart the centers of multiple Gaussian simulations are and how many Gaussians are within the range of spectral window. “Width” controls the width of each Gaussian function. “Distance” and “width” parameters were adjusted to optimize fitting. In this study, up to 3 Gaussian functions in the spectral window were used. For each fitting, the OPUS_RS returns a coefficient of correlation. Users have an option of setting a threshold of this coefficient. As noted in Table 1, OPUS_RS reports mixing ratios when the correlation coefficient of fitting is above this threshold. When the correlation is below this threshold, the pollutant is not “identified” and the mixing ratio is reported as zero.

The temperature dependence of the reference spectra was studied for CO , NH_3 , CO_2 and CH_4 . HITRAN spectra at 278 K, 298 K and 323 K were used in the OPUS_RS. One HITRAN spectrum at one of the three temperatures was loaded into the reference file which contained all the fitting information to produce a reference file for that temperature. The measurement conditions were set to 296 K and 101325 Pa in OPUS_RS, and measurement spectra were loaded by using the reference file at that temperature. The analysis was repeated by using reference files at three temperatures. After fitting the measurement spectra to reference spectra at the three temperatures, the difference in the extracted mixing ratio between

323 K and 278 K divided by the mixing ratio at 278 K was calculated. The maximum difference in retrieved mixing ratio for the 45 °C range was 8.9 % for NH₃, 4.2 % for CH₄, 8.3 % for CO, and 4.1 % for CO₂. This is a conservative estimate for the temperature related uncertainty, since the observed temperature range was much smaller than 45 °C.

Examples of measured spectra, fittings, and residuals are shown in Fig. S1.

S2. Scintillometer theory

The structure function of the optical refractive index C_n^2 is determined from the fluctuations of the light-beam intensities received by the scintillometer receiver. The structure parameter of temperature C_T^2 can be derived from C_n^2 given the ambient temperature, humidity, pressure, and wavelength (Thiermann and Grassl, 1992). The determination of the sensible heat flux H based on C_T^2 needs additional assumptions based on Monin-Obukhov Similarity Theory (MOST).

H is defined as

$$H = -\rho C_p \theta_* u_* \quad (S1)$$

where ρ is the air density, C_p is the specific heat capacity of air at constant pressure, θ_* is the temperature scale, and u_* is the friction velocity. θ_* and u_* are determined by the MOST functions (Wood et al., 2013):

$$\frac{C_T^2 z^{2/3}}{\theta_*^2} = \Psi_H \left(\frac{z}{L} \right) \quad (S2)$$

$$\frac{\kappa z U(z)}{\ln \left(\frac{z}{z_0} \right) u_*} = \Psi_M \left(\frac{z}{L} \right) \quad (S3)$$

where the Obukhov length L is defined as

$$L = \frac{T u_*^2}{\kappa g \theta_*} \quad (S4)$$

and z is the height above the surface, z_0 is the surface roughness length, the von Kármán constant $\kappa=0.4$, g is the gravitational constant, and U(z) is the mean horizontal wind speed. The scaling functions Ψ_H and Ψ_M can be calculated by Eqs. (S5) and (S6) (Thiermann and Grassl, 1992) and Eqs. (S7) (Paulson, 1970) and (S8) (Businger et al., 1971):

$$\Psi_H = 4\beta_1 \left[1 - 7 \frac{z}{L} + 75 \left(\frac{z}{L} \right)^2 \right]^{-1/3} \quad \text{for } \frac{z}{L} < 0 \quad (S5)$$

$$\Psi_H = 4\beta_1[1 - 7\frac{z}{L} + 20(\frac{z}{L})^2]^{1/3} \quad \text{for } \frac{z}{L} > 0 \quad (S6)$$

with $\beta_1=0.86$

$$\Psi_M = -2 \ln\left(\frac{1+\chi}{2}\right) - \ln\left(\frac{1+\chi^2}{2}\right) + 2 \arctan(\chi) - \frac{\pi}{2} \quad \text{for } \frac{z}{L} < 0 \quad (S7)$$

Where $\chi = (1 - 15\frac{z}{L})^{1/4}$

$$\text{and } \Psi_M = 4.7\frac{z}{L} \quad \text{for } \frac{z}{L} > 0 \quad (S8)$$

These calculations were performed with the software provided by Scintec (SRUN, version 1.31; see <http://www.scintec.com/english/web/scintec/Details/A012000.aspx>). The procedure to calculate the sensible heat flux H from measurements is as follows:

An initial $|L|=|L_{ini}| = 1000$ m is assumed, where the signs of L and H are determined by the simultaneous measurement of the vertical temperature gradient $\Delta T/\Delta z$. Then Ψ_H is calculated from Eqs. (S5) and (S6) using L and path height z. θ_* can then be calculated with C_T^2 using Eq. (S2). Next Ψ_M is calculated from Eqs. (S7) and (S8). Friction velocity u_* is then calculated by Eq. (S3) given the measured wind speed (from the NAPS station) and z_0 . A new L can then be calculated from Eq. (S4) using the calculated θ_* and u_* . This process is then repeated iteratively until the change in L is smaller than 0.1. Finally, H is calculated from Eq. (S1) using the last calculated values for θ_* and u_* . In the end, H, u_* and L were calculated at a 1-minute resolution in this study.

S3. Multi-year O₃ measurements from a regular NAPS station

It is also recognized that 2 weekends are not statistically enough to show the difference of O₃ mixing ratios between weekdays and weekends. The NAPS station which provided measurement results for this manuscript was a recently installed station, so it was there only for that summer. However, there is another nearby NAPS station (Station # 60430) which has been in operation for several years. NAPS station #60430 is located 175 m south of the highway 401 and about 200 m southwest of the NAPS research trailer in Fig.1. Therefore, we have extracted the O₃ mixing ratio from Station # 60430 for July and August from 2013 to 2015, to show some multi-year statistics. The diurnal variations of O₃ in July to August from 2013 to 2015 are shown in Fig. S7. The median of the diurnal average [O₃] on weekends from 7 am to midnight are higher than median on weekdays, which is consistent with the results from the new research NAPS trailer shown in the main text and Fig.9. There is no resolvable difference in 2013. Therefore, the difference between weekdays and weekends we observed in our 16-day measurement agrees with longer observations in 2014 and 2015, which suggests it is representative.

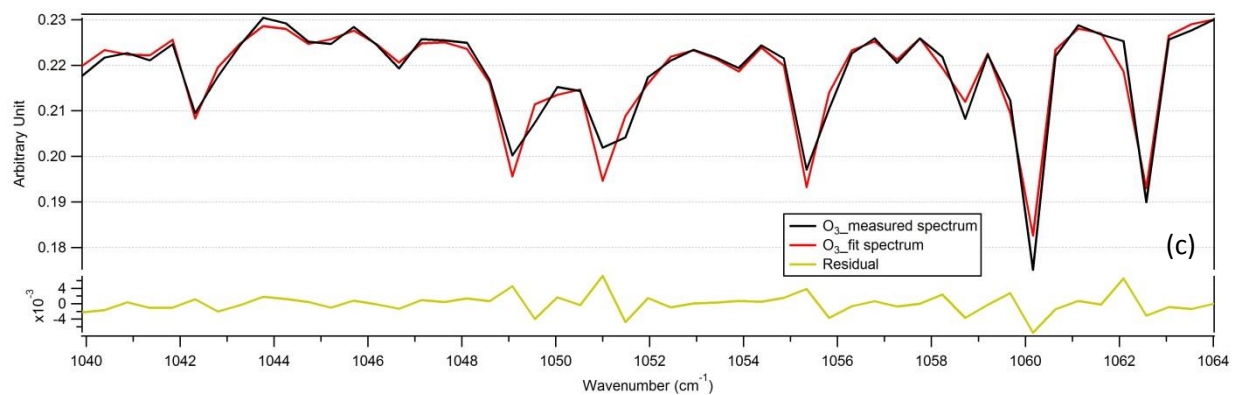
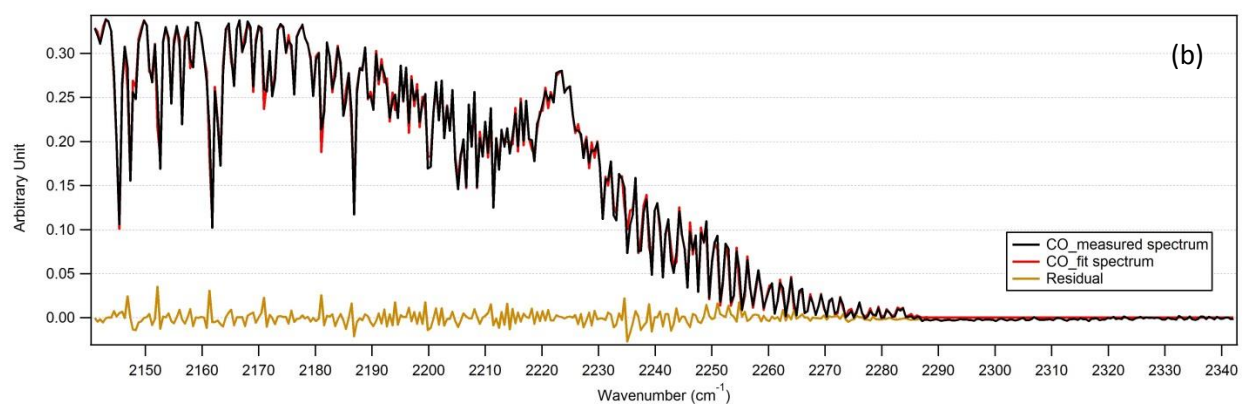
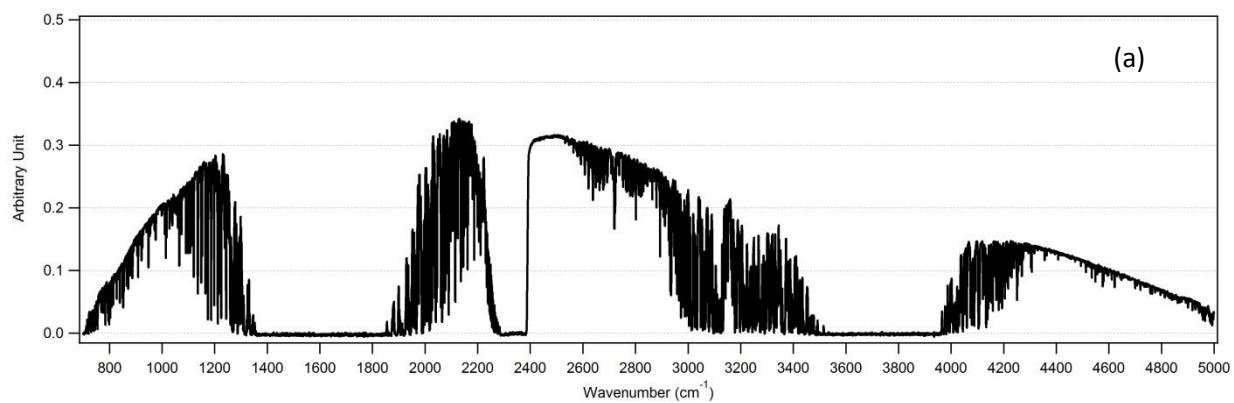
It is also interesting to compare the 2015 O₃ mixing ratio from the NAPS research trailer at the edge of highway with this regular NAPS station. The maximum median [O₃] on weekends (54 ppb) from the

trailer at edge was higher than median [O₃] at the regular station (50 ppb). Both stations show differences of 20 – 24 ppb in the median [O₃] between weekdays and weekends.

References

- Businger, J.A., Wyngaard, J.C., Izumi, Y. and Bradley, E.F.: Flux- profile relationships in the atmospheric surface layer, *J. Atmos. Sci.*, 28, 181-189, 1971.
- Harig, R., Rusch, P., Schäfer, K., Flores-Jardines, E.: "Method for on-site determination of the instrument line shape of mobile remote sensing Fourier transform spectrometers", *SPIE 5979*, 432-441, 2005.
- Paulson, C.A.: Mathematical representation of wind speed and temperature profiles in the unstable atmospheric surface layer, *J. Appl. Meteorol.*, 9, 857-861, 1970.
- Thiermann, V. and Grassl, H.: The measurement of turbulent surface-layer fluxes by use of bichromatic scintillation, *Bound-Lay. Meteorol.*, 58, 367-389, doi: 10.1007/BF00120238, 1992.
- Wood, C.R., Kouznetsov, R.D., Gierens, R., Nordbo, A., Järvi, L., Kallistratova, M.A. and Kukkonen, J.: On the temperature structure parameter and sensible heat flux over Helsinki from sonic anemometry and scintillometry, *J. Atmos. Ocean. Tech.*, 30, 1604-1615, doi: 10.1175/JTECH-D-12-00209.1, 2013.

Supplemental Figures



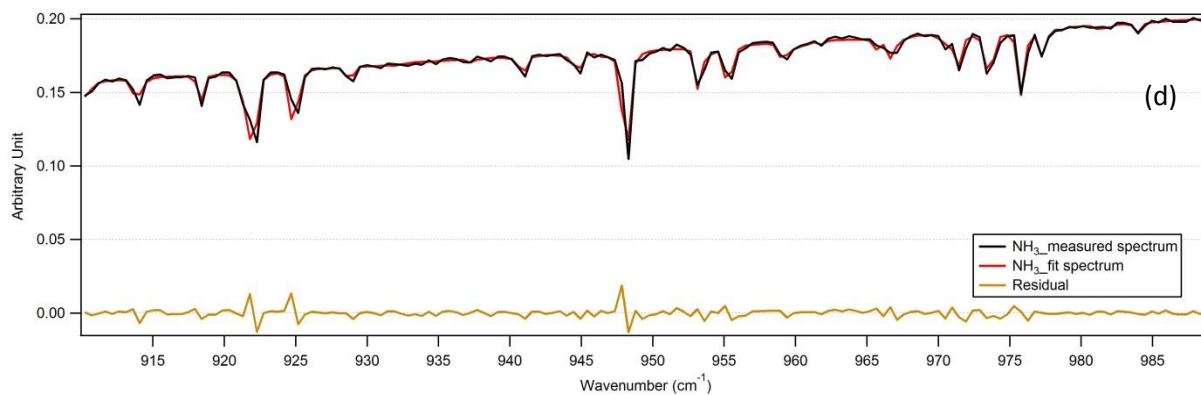


Figure S1: Examples of measured spectra at 16:01:45 on July 29, and fit modelled spectra made using the optimum spectral windows and OPUS_RS non-linear fitting method. The black curve is the measured spectrum; the red curve is the fit spectrum; and the brown curve is the residual. (a) full measured spectrum; (b) Spectral range for analysis of CO; (c) Spectral range for analysis of O₃; and (d) Spectral range for analysis of NH₃.

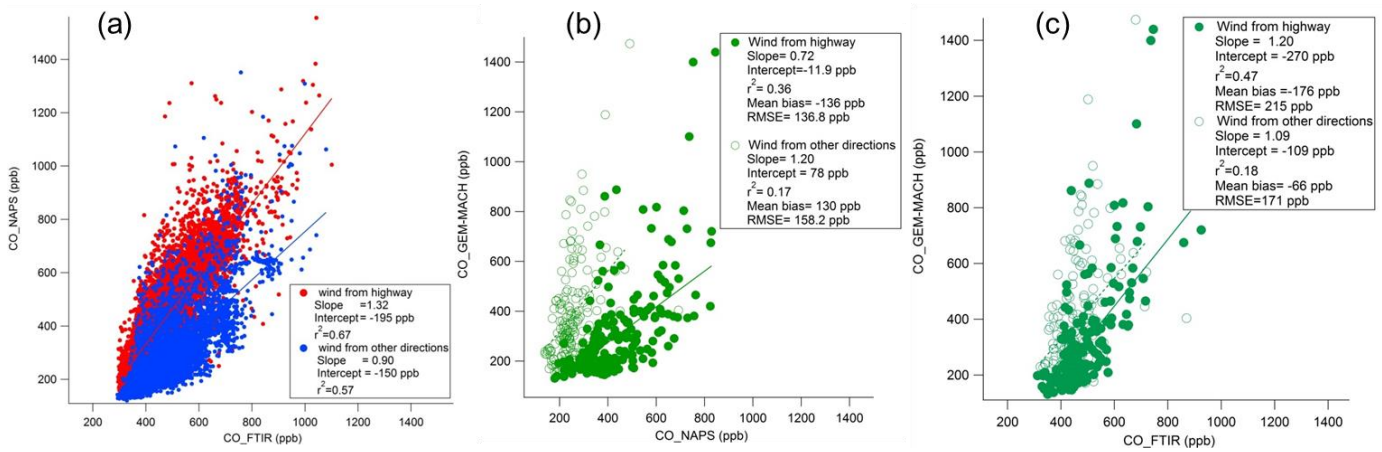


Figure S2: Comparison of CO mixing ratios: (a) NAPS and FTIR; (b) GEM-MACH and NAPS (c) GEM-MACH and FTIR. Red dots in (a) and solid circles in (b) and (c) show results when the wind was from the highway towards the NAPS trailer; Blue dots in (a) and open circles in (b) (c) show results when the wind was from other directions; the solid lines in (b) and (c) are the linear regression excluding 3 points when GEM-MACH results were much greater than measurement values; the dashed lines in (b) and (c) are the linear regression for these excluding the 4 most extreme outliers. Mean bias = [GEM_MACH]-[measurements]. RMSE = root mean square error.

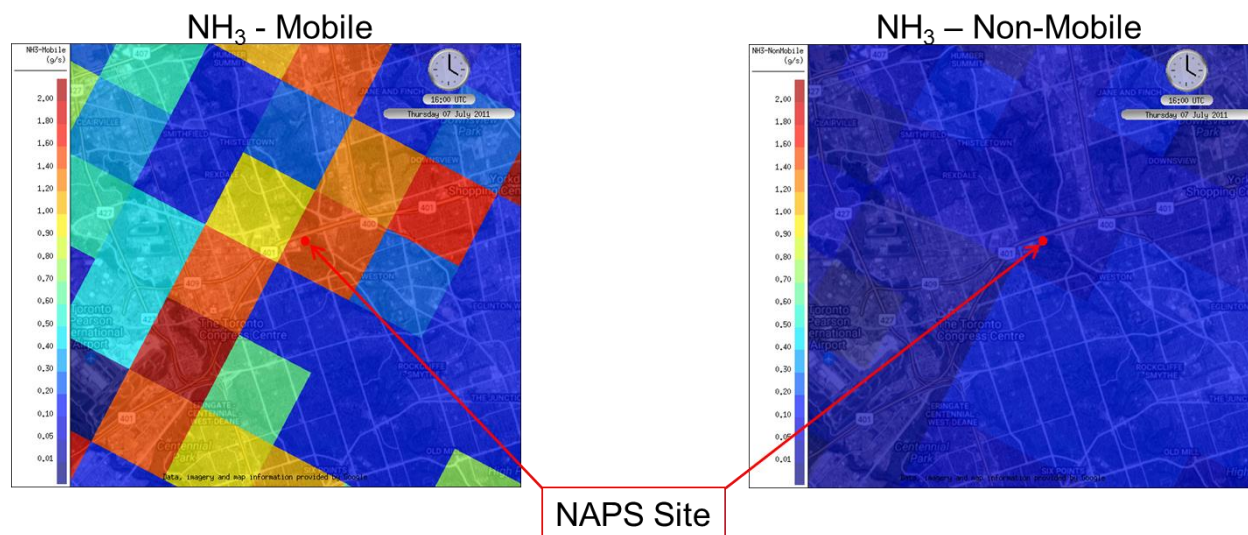


Figure S3: Gridded NH₃ emissions field used by GEM-MACH. Each grid cell is 2.5 km by 2.5 km in size, and the red dot marks the location of the NAPS trailer. The color scale indicates the magnitude of the emissions of NH₃ (g s⁻¹) in July 2010 from on-road mobile sources (left) and non-mobile sources (right).

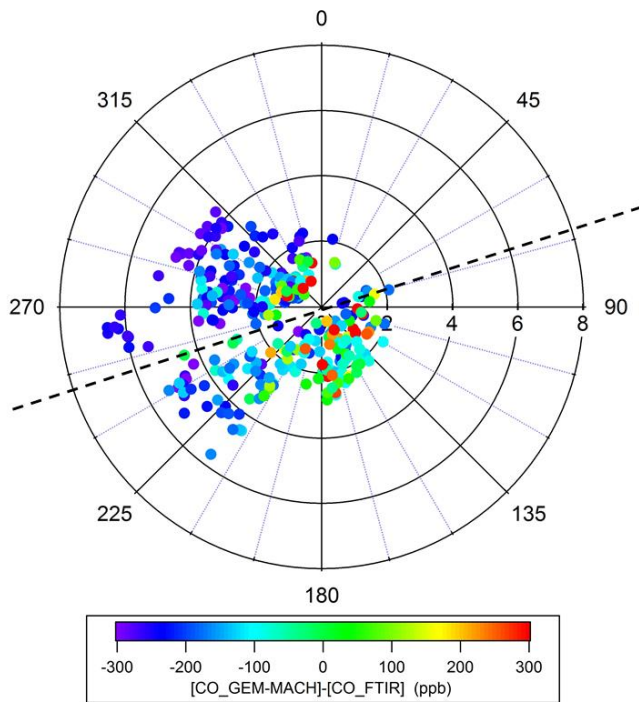


Figure S4: Polar plots of the difference of CO mixing-ratios between GEM-MACH output and FTIR measurements. Azimuth angle represents wind direction (meteorological convention), and radius indicates wind speed (m s^{-1}). The color indicates the CO mixing ratio difference. The center corresponds to the location of the NAPS trailer. The black dashed line shows the orientation of the highway: above this line, the wind came across the highway to the trailer.

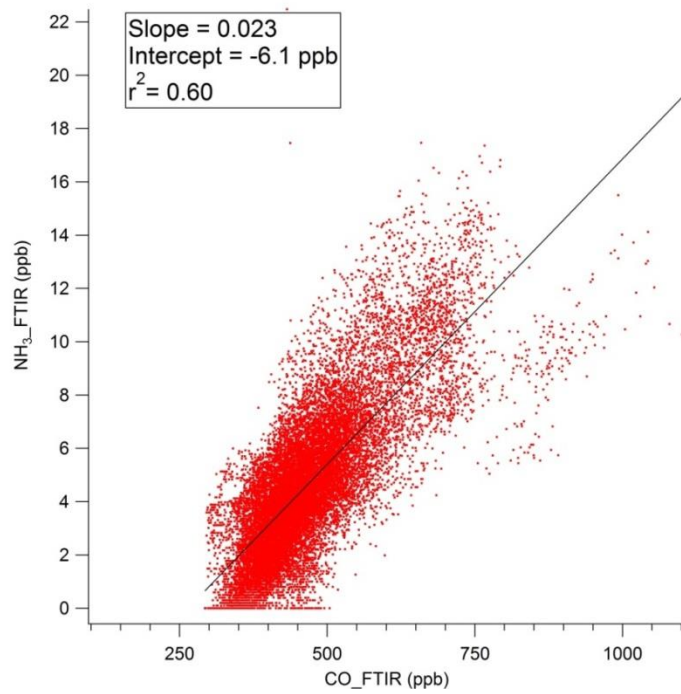


Figure S5: Linear relationship between NH₃ and CO mixing ratio from FTIR over the whole measurement period.

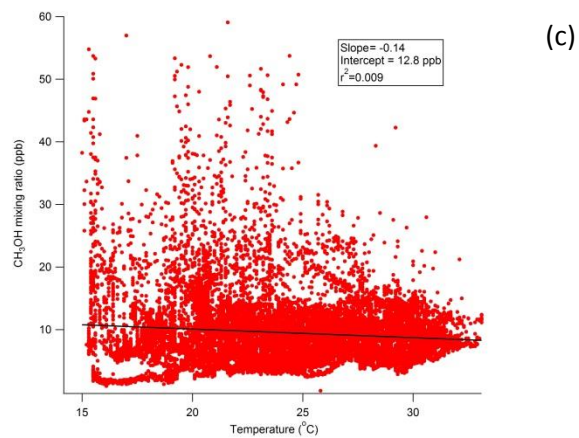
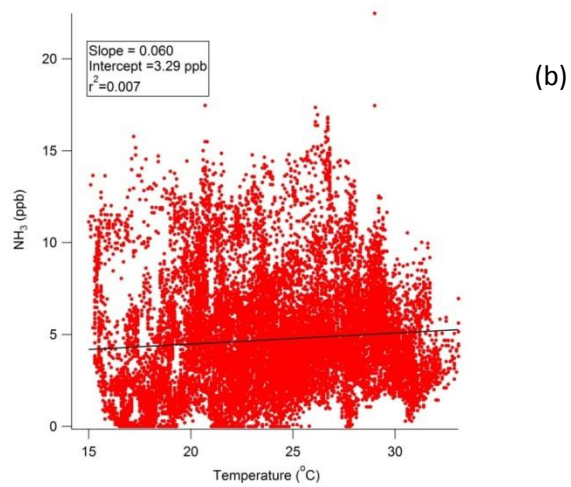
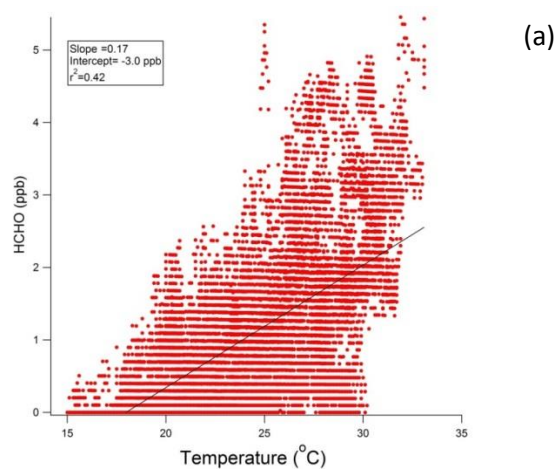


Figure S6: Correlation between mixing ratio of pollutants and ambient temperature for (a) HCHO; (b) NH₃; (c) CH₃OH

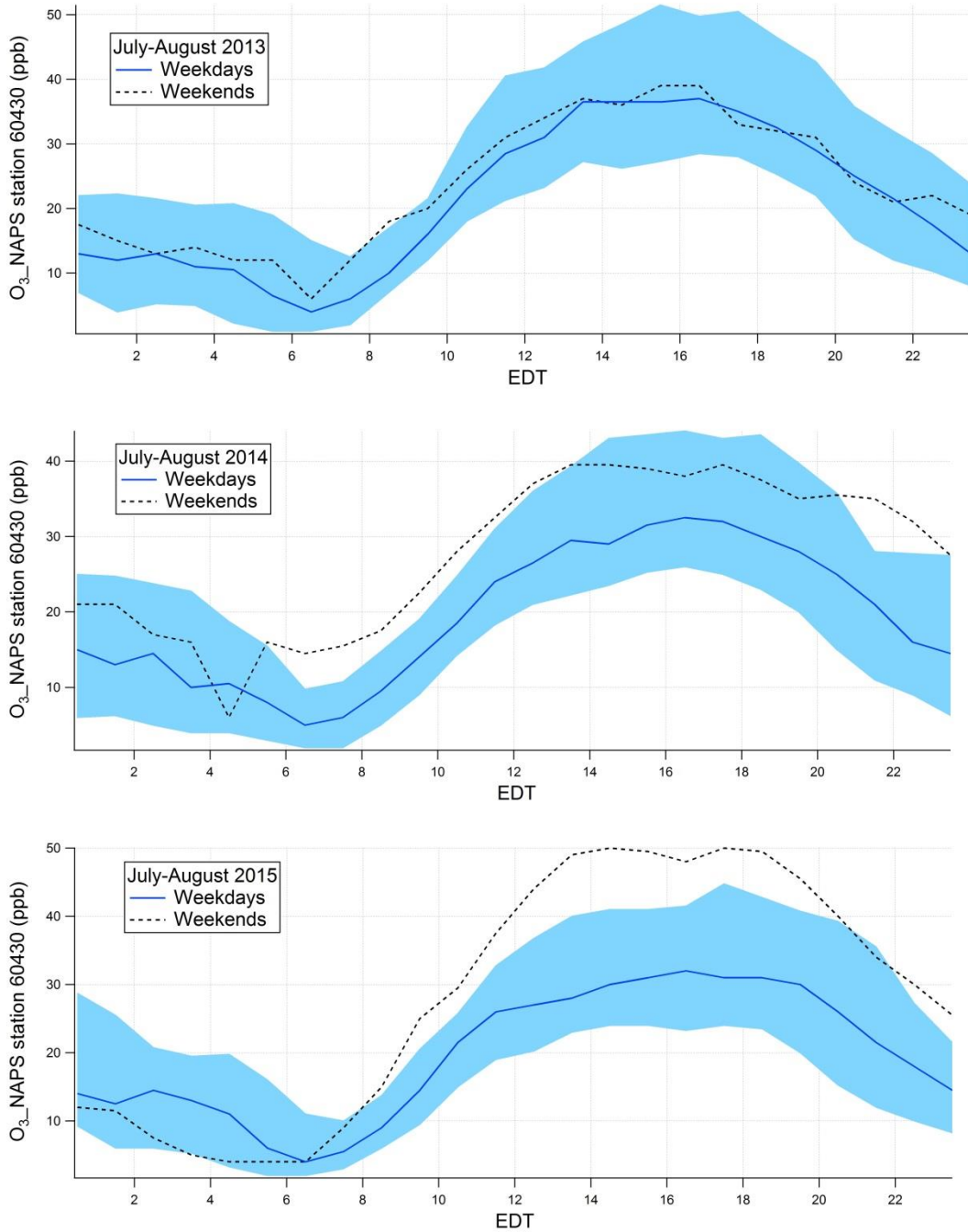


Figure S7: Average weekday and weekend diurnal cycles of mixing ratios of O₃ from NAPS station# 60430 in July-August 2013 (top), July-August 2014 (middle), and July-August 2015 (bottom). Solid blue lines are medians and the shaded areas are the interquartile ranges on weekdays; dashed black lines are medians on weekends.